



Discovery of novel hepatoselective HMG-CoA reductase inhibitors for treating hypercholesterolemia: A bench-to-bedside case study on tissue selective drug distribution

Jeffrey A. Pfefferkorn^{*}, John Litchfield, Richard Hutchings, Xue-Min Cheng, Scott D. Larsen, Bruce Auerbach, Mark R. Bush, Chitase Lee, Noe Erasga, Daniel M. Bowles, David C. Boyles, Gina Lu, Catherine Sekerke, Valerie Askew, Jeffrey C. Hanselman, Lisa Dillon, Zhiwu Lin, Andrew Robertson, Karl Olsen, Carine Boustany, Karen Atkinson, Theunis C. Goosen, Vaishali Sahasrabudhe, Jonathan Chupka, David B. Duignan, Bo Feng, Renato Scialis, Emi Kimoto, Yi-An Bi, Yurong Lai, Ayman El-Kattan, Rebecca Bakker-Arkema, Paul Barclay, Erick Kindt, Vu Le, Jaap W. Mandema, Mark Milad, Bradley D. Tait, Robert Kennedy, Bharat K. Trivedi, Mark Kowala

Pfizer Global Research & Development, Eastern Point Road, Groton, CT 06340, United States

ARTICLE INFO

Article history:

Received 8 October 2010
Revised 17 November 2010
Accepted 22 November 2010
Available online 26 November 2010

Keywords:

HMG-CoA reductase inhibitor
Statin
Hypercholesterolemia
Liver selective
Hepatoselective

ABSTRACT

The design of drugs with selective tissue distribution can be an effective strategy for enhancing efficacy and safety, but understanding the translation of preclinical tissue distribution data to the clinic remains an important challenge. As part of a discovery program to identify next generation liver selective HMG-CoA reductase inhibitors we report the identification of (3*R*,5*R*)-7-(4-((3-fluorobenzyl)carbamoyl)-5-cyclopropyl-2-(4-fluorophenyl)-1*H*-imidazol-1-yl)-3,5-dihydroxyheptanoic acid (**26**) as a candidate for treating hypercholesterolemia. Clinical evaluation of **26** (PF-03491165), as well as the previously reported **2** (PF-03052334), provided an opportunity for a case study comparison of the preclinical and clinical pharmacokinetics as well as pharmacodynamics of tissue targeted HMG-CoA reductase inhibitors.

© 2010 Elsevier Ltd. All rights reserved.

The tissue distribution of a drug can have significant impact on both its efficacy and safety and as a result there is interest in the development of small molecule therapeutics with selective tissue distribution profiles.¹ One area of particular focus is the design of hepatically-targeted agents given the liver's key role in metabolic regulation and the fact that it is the principal tissue affected by diseases such as hepatitis B and C viruses as well as hepatocellular carcinoma. Liver-targeted drug discovery approaches have been previously reported for diverse mechanistic classes such as HMG-CoA reductase inhibitors (i.e., statins),² glucocorticoid antagonists,³ thyroid hormone receptor agonists,⁴ glucokinase activators,⁵ stearyl-CoA desaturase inhibitors,⁶ hepatitis B and C antivirals,⁷ caspase inhibitors⁸ and nucleoside oncolytics.⁹ Among these examples, several strategies have been employed to achieve hepatoselectivity, including: (a) optimizing molecules for recognition and active uptake via liver specific transporters such as the organic anion transporting polypeptide (OATP) transporters and organic

cation transporters (OCT); (b) synthesizing conjugates with liver targeting motifs like bile acids or statins; and (c) designing prodrugs that undergo liver specific metabolic activation.^{2–4,7,9,10} A common issue when using either active transport processes or metabolic activation of prodrugs to achieve selective liver distribution is understanding the value and confidence of preclinical in vitro and in vivo models for predicting human drug distribution. In this report we describe a case study on the discovery of novel hepatoselective HMG-CoA reductase inhibitors, which provided an opportunity to compare preclinical transporter and drug distribution data with observed clinical pharmacokinetic and pharmacodynamic data.

Next generation HMG-CoA reductase inhibitors with enhanced hepatoselectivity relative to current statins offer promise for helping patients achieve increasingly aggressive LDL-reduction goals while minimizing the risk of myalgia, the muscle pain and weakness sometimes associated with statin therapy.² While the overall incidence of statin-induced myalgia is rather low (2–7% of patients), the probability of occurrence increases with drug dose, and it can be a key factor in reducing patient compliance with

^{*} Corresponding author. Tel.: +1 860 686 3421; fax: +1 860 715 4608.
E-mail address: jeffrey.a.pfefferkorn@pfizer.com (J.A. Pfefferkorn).

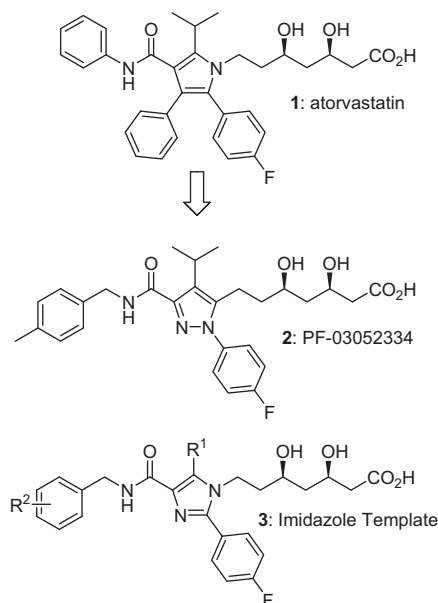


Figure 1. Structures of HMG-CoA reductase inhibitors.

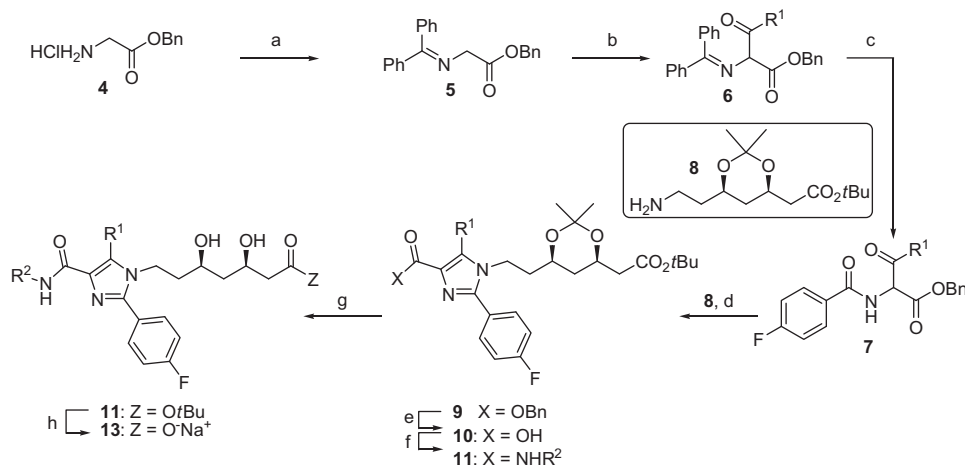
aggressive cholesterol treatment regimens.¹¹ Statin-induced myalgia is thought to involve, in part, inhibition of HMG-CoA reductase in non-hepatic tissues (particularly muscle) and accordingly it is hypothesized that its occurrence can be reduced by selectively targeting HMG-CoA reductase inhibitors to hepatic tissues and limiting peripheral exposure.¹¹ Moreover, it has been shown that this statin hepatoselectivity can be achieved by reducing inhibitor lipophilicity to minimize passive permeability into peripheral tissues while concurrently optimizing the molecules as substrates for active transport into hepatocytes.¹² In particular the OATP family of membrane transporters has been reported to be important for the selective liver distribution of statins as evidenced, in part, by the fact that patients with genetic variants in such transporters are at increased risk of statin-induced myalgia.¹³

As part of a discovery program to identify novel statins with best-in-class tolerability and efficacy through increased hepatoselectivity, we have investigated replacement of the pyrrole core of atorvastatin (**1**) with alternative five-membered heterocycles that offer reduced substitution and inherent lipophilicity as illustrated

in Figure 1. As previously reported, these efforts led to the discovery of pyrazole-based PF-03052334 (**2**) as a HMG-CoA inhibitor candidate.^{2e} To further improve upon the hepatoselectivity of **2**, we now report an extension of this strategy to imidazole-based HMG-CoA reductase inhibitors (i.e., **3**, Fig. 1). The synthesis and structure–activity studies of this imidazole-based series leading to clinical candidate selection will be described. Subsequently, we examine the preclinical transporter interactions, hepatocyte uptake, tissue distribution and biomarker response of this candidate as well as PF-03052334 (**2**) relative to their observed clinical data.

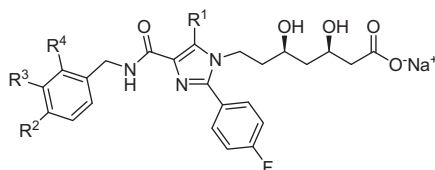
Scheme 1 illustrates the general synthesis of the inhibitors evaluated in these studies. A complete description of this synthesis has also been recently reported.¹⁴ Briefly, condensation of glycine benzyl ester hydrochloride (**4**, Scheme 1) with benzophenone imine afforded diphenyl imine **5** in high yield. Acylation of glycine diphenyl imine **5** with various acid chlorides (R¹COCl) at low temperature provided amine **6**, which upon treatment with 4-fluorobenzoyl chloride underwent conversion to keto amide **7**. Treatment of keto amide **7** with amine **8**¹⁵ at elevated temperature in the presence of AcOH and catalytic TsOH resulted in cyclization to form imidazole **9**. Subsequent hydrogenolysis of **9** to the corresponding carboxylic acid **10** and CDI-mediated coupling with amines (R²NH₂) provided amide **11**. Deprotection of the acetonide of **11** with TFA or HCl (aq) in MeOH followed by hydrolysis with NaOH provided the final product **13** as a sodium salt. The route outlined in Scheme 1 was utilized, with appropriate substitution of alternative building blocks, to prepare the analogs described in Table 1.

During structure–activity studies, compounds were initially screened in an HMG-CoA reductase enzyme inhibition assay from a rat microsomal preparation.¹⁶ Potent analogs were then evaluated for inhibition of cholesterol synthesis in both rat hepatocyte and rat myocyte cell lines with the ratio of these values (myocyte IC₅₀/hepatocyte IC₅₀) utilized as an assessment of cellular hepatoselectivity. Compounds were then evaluated in an in vivo hamster model measuring acute inhibition of cholesterol synthesis. In these experiments, animals were dosed po with 10 mg/kg inhibitor at *t* = 0 h then given an intraperitoneal injection of ¹⁴C sodium acetate at *t* = 2 h and blood samples were obtained at *t* = 4 h and analyzed for ¹⁴C cholesterol levels. These cholesterol levels were then compared to untreated control animals to determine percent inhibition of acute cholesterol synthesis. In several cases, in order to obtain a further assessment of a compound's



Scheme 1. General synthesis of substituted imidazoles as HMG-CoA reductase inhibitors. Reagents and conditions: (a) benzophenone imine, CH₂Cl₂, 20 °C, 8 h, 99%; (b) (i) KOtBu, R¹COCl, THF, –78 °C; (ii) HCl (aq); (c) 4-fluorobenzoyl chloride, Et₃N, CH₂Cl₂, 0 °C, 0.5 h; (d) **8**, xylene, AcOH, TsOH (cat), reflux, 16 h; (e) 10% Pd/C, H₂, MeOH, 25 °C, 4 h; (f) R²NH₂, CDI, DMF, 0–20 °C, 2 h; (g) TFA, CH₂Cl₂, 0 °C, 0.5 h or HCl (aq), MeOH, 45 °C, 12 h; (h) NaOH (aq), THF, 50 °C, 2 h.

Table 1
Structure and biological activity of substituted imidazole analogs **14–33**



	R ¹	R ²	R ³	R ⁴	HMG-CoA ^a IC ₅₀ (nM)	Cellular inhibition of cholesterol synthesis ^b			In vivo inhibition of cholesterol synthesis ^b		Log D ^c (pH 7.4)
						Hepatocyte IC ₅₀ (nM)	Myocyte IC ₅₀ (nM)	Cell Selectivity	(10 mg/kg)		
									t = 2–4 h	t = 3–5 h	
2					1.0	0.9	730	810	–74%	–	0.24
Rosuvastatin					3.1	0.3	250	830	–76%	–	1.01
14	Me	H	H	H	94	–	–	–	–	–	–
15	Et	H	H	H	123	–	–	–	–	–	–
16	nPr	H	H	H	26	–	–	–	–	–	–
17	iPr	H	H	H	7.9	0.3	3030	10,100	–53%	–7%	0.64
18	cPr	H	H	H	1.4	0.2	632	3160	–58%	–	0.03
19	cPr	Me	H	H	1.7	0.1	178	1780	–79%	–36%	0.45
20	cPr	H	Me	H	7.2	0.3	532	1770	–54%	–50%	0.47
21	cPr	H	H	Me	4.9	0.1	4850	48,500	–	0%	0.44
22	cPr	OMe	H	H	1.2	0.2	6400	32,000	–60%	–	0.02
23	cPr	H	OMe	H	1.2	0.2	538	2960	–53%	–42%	0.11
24	cPr	H	H	OMe	7.0	0.1	10,700	107,000	–	–	0.16
25	cPr	F	H	H	3.4	0.7	1620	2310	–	0%	0.17
26	cPr	H	F	H	1.2	0.1	444	4440	–68%	–43%	0.51
27	cPr	H	H	F	1.5	ND	27,200	–	–	–4%	0.08
28	cPr	F	F	H	1.2	0.5	2780	5560	–	–8%	–
29	cPr	F	H	F	1.2	0.2	4870	24,350	–46%	–	–
30	cPr	Me	F	H	4.1	0.1	224	2240	–	–	0.69
31	cPr	OMe	F	H	3.7	0.2	890	4450	–36%	0%	–
32	cPr	C(O)NH ₂	H	H	7.2	0.4	>100,000	>250,000	–	0%	–1.1
33	cPr	SO ₂ NMe ₂	H	H	4.9	0.5	>100,000	>200,000	–	0%	–0.46

^a In vitro assay values reported as the mean ± SEM of $n \geq 2$ independent determinations.

^b Data represent the mean of the percent change from the control group ($n = 8$ /group).

^c Log D determined by shake flask method.

duration of action, the experiment was repeated with later timepoints in separate animal groups with drug dosing at $t = 0$ h, ¹⁴C sodium acetate injection at $t = 3$ h and cholesterol level determination at $t = 5$ h.

As shown in Table 1, initial structure–activity efforts focused on evaluating the effect of the R¹ imidazole substituent. As shown for compounds **14–18**, inhibitory potency increased with increasing substituent size with cPr > iPr > nPr > Et ~ Me. Among these analogs, both **17** (R¹ = iPr) and **18** (R¹ = cPr) offered sufficient in vitro potency to warrant selectivity and efficacy testing. Encouragingly, the cellular hepatoselectivity ratios for **17** (10,100×) and **18** (3160×) were significantly greater than that of **2** (810×) or rosuvastatin (830×); however, on the downside both **17** and **18** demonstrated reduced acute in vivo efficacy relative to these same benchmarks.

We next examined the effects of substituents on the benzamide with the goal of increasing efficacy while maintaining cellular hepatoselectivity. Given the moderate improvement in vitro potency offered by **18** over **17**, these studies were conducted in the R¹ = cPr series. As highlighted in Table 1, several trends were observed during these studies. First, introduction of a 4-Me (**19**), 3-Me (**20**), 3-OMe (**23**) or 3-F (**3**) offered optimal effects on magnitude and duration of in vivo inhibition of cholesterol synthesis relative to the unsubstituted case (i.e., **18**) while still maintaining the hepatoselectivity. Second, for cases where a complete ortho, meta, and para substitution pattern was explored (e.g., **19**, **20**, **21**) cellular hepatoselectivity tended to be optimal with ortho substitution (**21** > **19**, **20**) but, in contrast, in vivo efficacy tended to be

optimal with substitution in either the para or meta position (**19** > **20** > **21**). Third, efforts to combine optimal substituents (4-Me, 4-OMe, 3-F) from the monosubstituted analogs into disubstituted analogs such as **30** and **31** generally did not afford additive potency or efficacy. Finally, as shown for **32** and **33** introduction of increasingly polar substituents resulted in analogs with significantly increased cellular hepatoselectivity but no in vivo efficacy presumably due to the very poor passive membrane permeability of these analogs as suggested by their significantly lower measured Log D values.

Among the imidazole analogs evaluated, compound **26** was selected for further characterization based on its favorable balance of hepatoselectivity and in vivo efficacy. Specifically, the cellular hepatoselectivity (4440×) of **26** offered a fivefold improvement relative to either rosuvastatin or **2** and the compound had comparable acute in vivo efficacy for inhibition of cholesterol synthesis. To further characterize its efficacy, **26** was then evaluated in a 7-day LDL lowering dose–response study conducted in chow-fed guinea pigs as shown in Figure 2.¹⁶ For comparison, rosuvastatin and pravastatin were included as benchmarks representing the current standard of care statins with the highest levels of hepatoselectivity. As illustrated, the ED₅₀ of **26** was 5.9 mg/kg with an E_{max} similar to rosuvastatin, but less than that of compound **2**.

The comparative pharmacokinetics and tissue distribution properties of **2** and **26** were next characterized in preclinical species. Plasma and tissue protein binding properties were characterized as shown in Table 2 wherein compound **2** was found to be approximately 10-fold more protein bound than **26**.

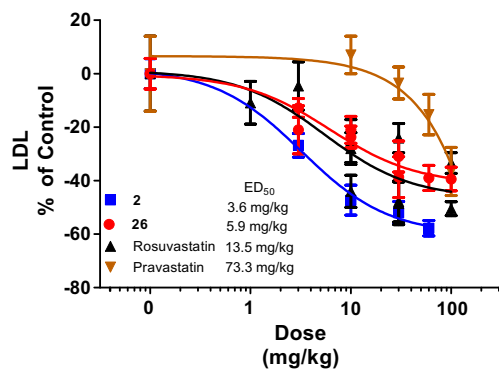


Figure 2. Dose–response effect of **26** on plasma low density lipoprotein (LDL) in the Guinea pig. Animals were dosed with **2**, **26**, pravastatin or rosuvastatin for seven days. All groups were sacrificed 2 h post dose on the final day of dosing. Data represent the mean \pm SEM of the percent change from the control group ($n = 8$ /group).

Table 2
Protein binding properties of selected HMG-CoA inhibitors

Compd	Rat plasma f_u	Rat liver f_u	Dog plasma f_u	Human plasma f_u
2	0.016	0.052	0.032	0.051
26	0.15	0.23	0.43	0.29
Rosuvastatin	0.06	0.17	ND	0.17

Plasma protein binding value determined at 0.5 μ g/mL. Liver tissue protein binding values determined at 1 μ M.

As summarized in Table 3, rat and dog pharmacokinetics studies revealed both **2** and **26** to have moderate systemic plasma clearance, low volume of distribution and relatively low bioavailability (particularly for **26**) consistent with the preclinical profiles of other statins. Evaluation of clearance mechanisms in rat revealed biliary excretion of parent as the primary clearance pathway for both compounds with negligible contributions from renal clearance or oxidative metabolism. Separately, since certain statins are known to form side-chain lactones (i.e., closure of C-3 hydroxyl with carboxylate) under physiological conditions, during these rat and dog PK studies of **2** and **26** plasma samples of were concurrently analyzed for the corresponding lactones.¹⁷ While such lactones are intrinsically inactive against HMG-CoA reductase, there is a possibility that circulating levels of these more permeable lactone forms may distribute to non-hepatic tissues where reconversion to the active acid form could occur thus reducing the apparent hepatoselectivity of an inhibitor.¹⁷ In both rat and dog there were no detectable lactone concentrations found for compound **26**. For compound **2** plasma lactone levels were found to

Table 3
Preclinical pharmacokinetics studies for **2** and **26** in rat and dog

Compd	Dose (mg/kg)	AUC _(0–24) ^a (ng * h/mL)	C _{max} ^a (ng/mL)	Cl (mL/min/kg)	T _{1/2} (h)	Vd _{ss} (L/kg)	%F
2	Rat iv	10	–	27	0.34	0.14	–
2	Rat po	6.4	1.3	–	–	–	6%
2	Dog iv	28	–	19	0.78	0.10	–
2	Dog po ^b	64	51.5	–	–	–	44%
26	Rat iv	83	–	39	0.43	0.17	–
26	Rat po	2.7	2.0	–	–	–	0.3%
26	Dog iv	293	–	25	0.27	0.10	–
26	Dog po ^c	51	5.4	–	–	–	2.2%

Pharmacokinetic parameters expressed as geometric mean of $n = 2$ animals per group unless otherwise noted.

^a AUC_(0–24) and C_{max} reported as free drug concentration using plasma protein binding values determined in Table 3.

^b $n = 3$.

^c $n = 1$.

be 0.04- and 1.7-fold of the parent acid concentration in dog and rat, respectively.

To better understand the underlying transport mechanism responsible for the distribution of these HMG-CoA reductase inhibitors we examined their uptake in sandwich-cultured rat and human hepatocytes as summarized Tables 4 and 5, respectively. In rat hepatocytes, the active uptake rates were similar for the three molecules and uptake was inhibited by rifamycin SV as a pan-OATP inhibitor. In human hepatocytes, the active uptake rates were similar for **2** and rosuvastatin but somewhat lower for **26**. Similar to rat hepatocytes, the active uptake of all three compounds was significantly inhibited in the presence of rifamycin SV. To further understand the mechanism of hepatic active uptake, the three HMG-CoA reductase inhibitors were then evaluated as a potential substrate for rat (Table 4) and human (Table 5) hepatic OATP transporters. In these assays, individual rat (rOatp1a1, rOatp1a4 and rOatp1b2) and human transporters (hOATP1B1, hOATP1B3 and hOATP2B1) were over expressed in CHO-cells or HEK293 cells enabling determination of the fold difference in substrate uptake relative to the wild type cell line for each transporter.¹⁸ Rosuvastatin/pravastatin and midazolam served as positive and negative controls, respectively, in each assay. Both **26** and **2** were found to be substrates for rOatp1a1, rOatp1a4 and rOatp1b2 transporters as well as human hOATP1B1 and hOATP1B3. Compound **26** also appeared to be a weak substrate for hOATP2B1. Qualitatively, **2** and **26** were found to undergo similar uptake via the rat transporters, but **26** was suggested to be a stronger substrate for the corresponding human transporters. Moreover, in the human hepatocyte uptake assay (Table 5, left side) uptake of **26** was found to be 97% active versus 78% active for **2**, further suggesting that **26** was potentially a better substrate for human hepatic uptake.

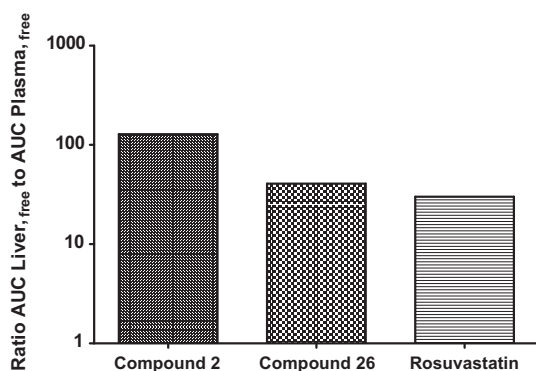
Having determined **2** and **26** to be in vitro substrates for hepatic transporters, we next evaluated their in vivo liver distribution and pharmacokinetic/pharmacodynamic (PK/PD) profiles. Oral dosing of **2**, **26** and rosuvastatin to rats followed by sacrifice and determination of free plasma and liver drug concentration at regular intervals ($t = 0, 0.5, 1, 2, 3, 4, 7$ and 24 h) enabled calculation of liver/plasma AUC_(0–24h) ratios. As summarized in Figure 3, all three exhibited enhanced liver-to-plasma drug concentrations. The liver-to-plasma ratios were 41 \times , 128 \times and 30 \times for **26**, **2** and rosuvastatin, respectively. Given that a similar direct determination of liver drug exposures during clinical studies was not feasible, we sought a circulating biomarker measurement of hepatic inhibition of HMG-CoA reductase that could be used as a surrogate using a PK/PD relationship. Mevalonate (MVA) was selected for this purpose since it is the direct product of HMG-CoA reductase.¹⁹ The liver is the major site of MVA production with approximately 1% reaching systemic circulation. These plasma MVA concentrations have been shown to closely correlate with hepatic cholesterol

Table 4Evaluation of transporter mediated uptake of **2**, **26** and rosuvastatin in rat hepatocytes and transfected cells expressing rat transporters¹⁸

Compound	Concn (μM)	Rat hepatocyte uptake rates ^a		Rat transporters fold uptake ^b		
		Rate (pmol/min/mg protein)	% Inhibitible ^c	rOatp1a1	rOatp1a4	rOatp1b2
2	1	14	98%	3.6	2.7	2.9
2	10	–	–	4.2	3.0	2.6
26	1	17	100%	5.8	4.4	1.8
26	10	–	–	4.4	7.3	1.7
Rosuvastatin ^d	1	24	97%	8.2	8.6	–
Rosuvastatin	10	–	–	5.3	17.3	–
Pravastatin ^d	1	–	–	2.4	1.5	3.6
Pravastatin	10	–	–	3.9	1.8	7.0
Midazolam ^e	1	–	–	1.6	0.93	1.1
Midazolam	10	–	–	1.7	0.82	1.3

^a Determined in rat hepatocytes cultured in sandwich configuration using BioCoat plates with Matrigel overlay.^b Conducted in transfected CHO or HEK cells.^c Inhibition by pan OATP inhibitor rifamycin SV.^d Positive control.^e Negative control.**Table 5**Evaluation of transporter mediated uptake of **2**, **26** and rosuvastatin in human hepatocytes and transfected cells expressing human transporters

Compound	Concn (μM)	Human hepatocyte uptake rates ^a		Human transporters fold uptake ^b		
		Rate (pmol/min/mg protein)	% Inhibitible ^c	hOATP1B1	hOATP1B3	hOATP2B1
2	1	7.8	78%	21.6	11.1	2.1
2	10	–	–	18.4	5.0	1.4
26	1	1.5	97%	49.0	34.5	7.1
26	10	–	–	84.9	36.4	6.8
Rosuvastatin ^d	1	8.0	85%	14.4	3.7	5.5
Rosuvastatin	10	–	–	69.6	11.1	6.6
Pravastatin ^d	1	–	–	73.7	13.0	–
Pravastatin	10	–	–	223	32.8	–
Midazolam ^e	1	–	–	0.6	0.9	0.8
Midazolam	10	–	–	0.9	1.1	0.7

^a Determined in human hepatocytes cultured in sandwich configuration using BioCoat plates with Matrigel overlay.^b Conducted in transfected CHO or HEK cells.^c Inhibition by pan OATP inhibitor rifamycin SV.^d Positive control.^e Negative control.**Figure 3.** Liver-to-plasma distribution of **2** (25 mg/kg), **26** (10 mg/kg) and rosuvastatin (10 mg/kg) after single oral dose in Sprague-Dawley rats. Ratios were determined based on $\text{AUC}_{(0-24\text{h})}$ of free drug concentrations in liver and plasma. Time points were samples at $t = 0, 0.5, 1, 2, 3, 4, 7$ and 24 h with $n = 3$ animals per time point.

synthesis making it an attractive circulating biomarker for evaluating the hepatic action of HMG-CoA reductase inhibitors.²⁰ To establish a preclinical PK/PD relationship, during the drug tissue distribution studies described in Figure 3, the plasma levels of

mevalonic acid were concurrently measured at each time point. Figure 4 illustrates the time course for both plasma drug (Panel A) and MVA (Panel B) concentrations during this experiment. While compound **26** exhibited the lowest plasma concentrations it also offered the most significant and sustained reduction in the MVA biomarker relative to either **2** or rosuvastatin with a notable 47% MVA reduction even at 24 h post dose. This property of **26** is further illustrated in PK/PD analysis (Panel C) where plotting plasma drug exposure versus MVA reduction suggests that **26** achieves comparable levels of MVA reduction relative to **2** or rosuvastatin but does so at lower systemic drug concentrations. This observation, coupled with the data of a more sustained MVA reduction observed with **26** in time course studies (i.e., Fig. 4, Panel B), may suggest that, in rat, **26** achieves a more favorable balance of hepatic uptake and efflux relative to the other inhibitors. Interestingly, this PK/PD data (Fig. 4, Panel C) which indicates **26** to be more functionally hepatoselective than **2** somewhat contrasts the previous liver/plasma drug distribution data (Fig. 3) which indicated that **2** achieved a greater ($128\times$ vs $41\times$) liver-to-plasma free drug ratios.

Based on promising efficacy and preclinical safety data, both **2** (PF-03052334)²¹ and **26** (PF-03491165) were advanced to Phase 1 ascending single dose studies in healthy volunteers to evaluate the human safety and pharmacokinetics of these novel statins. This dose escalation also offered an opportunity to evaluate human

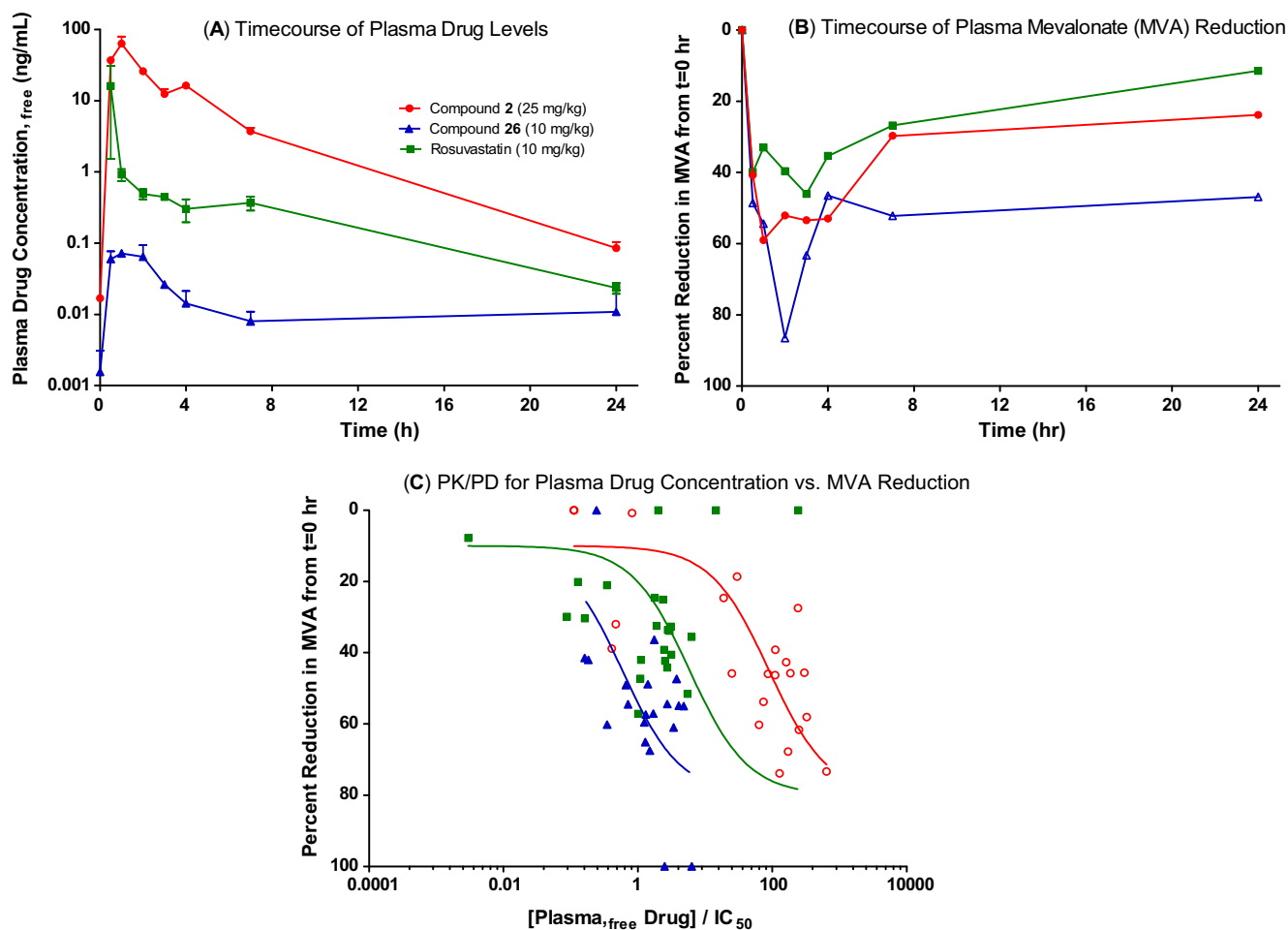


Figure 4. Plasma drug levels (A), plasma mevalonate (MVA) changes (B) and exposure effect relationships (C) for **2**, **26** and rosuvastatin in Sprague-Dawley rats.

pharmacodynamics via mevalonate (MVA) changes as summarized in Table 6. Both compounds were well tolerated, and demonstrated relatively dose-proportional increases in drug exposure. Inhibitor **2** had a terminal half-life of 6–9 h with 12–16% of drug excreted in the urine at 24 h post dose. Inhibitor **26** had a terminal half-life of 4–7 h with <1% of drug excreted in the urine at 24 h post dose. At C_{\max} plasma lactone levels of **2** averaged 0.08-fold of the parent

acid concentration whereas plasma lactone levels of **26** averaged twofold of the parent acid concentration.

MVA biomarker measurements revealed dose-dependent decreases both for **2** and **26**. For example, at a dose of 120 mg, **26** achieved a plasma C_{\max} of 3.31 ng/ml resulting in a decrease in plasma mevalonate $AUC_{(0-24h)}$ of 46% whereas a dose of 80 mg of **2** achieved plasma C_{\max} of 3152 ng/ml resulting in a decrease in

Table 6
Human pharmacokinetics and mevalonate (MVA) changes for Phase 1 single ascending dose studies of **2** and **26** in human volunteers

Compd	Dose (mg)	N	$t_{1/2}^a$ (h)	Plasma exposures total drug ^b		Plasma exposures free drug ^c		Mean% change plasma MVA relative to placebo control ^d	
				C_{\max} (ng/mL)	$AUC_{(0-\infty)}$ (ng * h/mL)	C_{\max} (ng/mL)	$AUC_{(0-\infty)}$ (ng * h/mL)	$AUC_{(0-24h)}$	$AUC_{(0-72h)}$
2	1	6	2.55 (33)	33.5 (27)	78.5 (30)	1.71	4.00	-16 ± 27	-8 ± 25
	5	6	4.54 (31)	196 (27)	434 (32)	10.0	22.1	-13 ± 32	+3 ± 14
	20	6	5.27 (42)	740 (28)	1930 (21)	37.7	98.4	-34 ± 7	-17 ± 11
	40	6	8.57 (46)	1770 (24)	5110 (31)	90.3	261	-41 ± 14	-3 ± 17
	80	5	6.28 (23)	4480 (12)	11,800 (9)	228	602	-65 ± 5	-29 ± 21
	160	6	8.87 (45)	6810 (27)	25,000 (23)	347	1280	-55 ± 16	-24 ± 22
6	3	6	—	0.0552 (245)	—	0.016	—	-5 ± 23	-10 ± 21
	10	6	—	0.355 (202)	2.71	0.103	0.786	-25 ± 10	-13 ± 10
	40	6	3.22 (39)	2.25 (94)	6.27 (83)	0.653	1.81	-39 ± 19	-19 ± 16
	120	6	3.07 (69)	3.31 (90)	12.5 (91)	0.960	3.63	-46 ± 9	-17 ± 19
	240	5	4.06	9.27 (58)	27.2 (58)	2.69	7.89	-56 ± 12	-30 ± 31
	320	6	7.36 (156)	44.1 (121)	36.0 (79)	12.8	10.4	-61 ± 11	-28 ± 37

^a Terminal half-life ($t_{1/2}$) reported as arithmetic mean (%CV).

^b C_{avg} and $AUC_{(0-\infty)}$ values reported as arithmetic mean (%CV) of total drug levels for parent carboxylic acid.

^c C_{avg} and $AUC_{(0-\infty)}$ values reported as free drug levels for parent carboxylic acid using protein binding values reported in Table 3.

^d Percent change from placebo ± standard deviation of plasma mevalonic acid.

plasma mevalonate AUC_(0–24h) of 65%. For comparison, in a separate study, once daily dosing of 10 mg of rosuvastatin for 14 days in healthy volunteers resulted in a 29.9% decrease in plasma mevalonate AUC_(0–24h) accompanied by a 41.3% reduction in LDL-C with a plasma C_{max} of 4.58 ng/ml for this benchmark statin.²²

From the perspective of drug distribution, while **2** and **26** achieved similar pharmacodynamic effects (i.e., MVA reductions) they were achieved at significantly different systemic drug exposures based on either free or total drug as shown in Table 6. For example, at the highest doses of each compound which offered comparable MVA reductions, the systemic free drug concentrations of **2** at C_{max} were 27-fold higher than for **26**. This may suggest that in humans **26** undergoes more efficient hepatic extraction than **2** and also has sufficient liver residency time to induce a sustained reduction in hepatic cholesterol synthesis. Presumably, the lower systemic drug levels observed for **26** may offer the potential for side effects reduced effects, such as myalgia, that occur as a result of non-hepatic inhibition of HMG-CoA reductase. This clinical observation of efficacy at lower systemic drug concentrations of **26** versus **2** was consistent with the preclinical PK/PD trend observed in rat (Fig. 4, Panel C) as well as the in vitro transporter data suggesting that **26** (vs **2**) was a more effective substrate for the human hOATP1B1, hOATP1B3 and hOATP2B1 transporters (Table 5). Interestingly, the sandwich-cultured human hepatocyte uptake data did not predict the increased hepatic uptake rate of **26** versus **2**.

We have described the structure–activity studies leading to the identification of hepatoselective HMG-CoA reductase inhibitor **26** as an early clinical candidate for treating hypercholesterolemia. The comparative preclinical profiling of imidazole-based **26** versus pyrazole-based inhibitor **2** highlighted interesting differences in transporter interactions, tissue distribution and lactone formation between these structurally similar candidates. The prediction of tissue selective drug distribution remains an important drug discovery challenge, and in the current case study preclinical hepatic transporter assays and a PK/PD analysis of systemic drug concentration versus hepatic pharmacodynamic effects offered insight useful for predicting the rank order (**26** > **2**) of hepatoselectivity observed in early clinical studies of these candidates.

References and notes

- For reviews, see: (a) Lin, J. H. *Curr. Drug Metab.* **2006**, *7*, 39; (b) Lanao, J. M.; Fraile, M. A. *Curr. Pharm. Des.* **2005**, *11*, 3829; Mizuno, N.; Niwa, T.; Yotsumoto, Y.; Sugiyama, Y. *Pharmacol. Rev.* **2003**, *55*, 425.
- For a review, see: (a) Pfefferkorn, J. A. *Curr. Opin. Invest. Drugs* **2009**, *10*, 245; For representative examples, see: (b) Koga, T.; Shimada, Y.; Kuroda, M.; Tsujita, Y.; Hasegawa, K.; Yamazaki, M. *Biochim. Biophys. Acta* **1990**, *1045*, 115; (c) Roth, B. D.; Bocan, T. M.; Blankey, C. J.; Chucholowski, A. W.; Creger, P. L.; Creswell, M. W.; Ferguson, E.; Newton, R. S.; O'Brien, P.; Picard, J. A.; Roark, W. H.; Sekerke, C. S.; Sliskovic, D. R.; Wilson, M. W. *J. Med. Chem.* **1991**, *34*, 463; (d) Ahmad, S.; Madsen, C. S.; Stein, P. D.; Janovitz, E.; Huang, C.; Ngu, K.; Bisaha, S.; Kennedy, L. J.; Chen, B. C.; Zhao, R.; Sitkoff, D.; Monshizadegan, H.; Yin, X.; Ryan, C. S.; Zhang, R.; Giancarli, M.; Bird, E.; Chang, M.; Chen, X.; Setters, R.; Search, D.; Zhuang, S.; Nguyen-Tran, V.; Cuff, C. A.; Harrity, T.; Darienzo, C. J.; Li, T.; Reeves, R. A.; Blonar, M. A.; Barrish, J. C.; Zahler, R.; Robl, J. A. *J. Med. Chem.* **2008**, *51*, 2722; (e) Pfefferkorn, J. A.; Choi, C.; Larsen, S. D.; Auerbach, B.; Hutchings, R.; Park, W.; Askew, V.; Dillon, L.; Hanselman, J. C.; Lin, Z.; Lu, G. H.; Robertson, A.; Sekerke, C.; Harris, M. S.; Pavlovsky, A.; Bainbridge, G.; Caspers, N.; Kowala, M.; Tait, B. D. *J. Med. Chem.* **2008**, *51*, 31.
- (a) von Geldern, T. W.; Tu, N.; Kym, P. R.; Link, J. T.; Jae, H.-S.; Lai, C.; Apelqvist, T.; Rhonstad, P.; Hagberg, L.; Koehler, K.; Grynfarb, M.; Goos-Nilsson, A.; Sandberg, J.; Österlund, M.; Barkhem, T.; Höglund, M.; Wang, J.; Fung, S.; Wilcox, D.; Nguyen, P.; Jakob, C.; Hutchins, C.; Färnegardh, M.; Kauppi, B.; Öhman, L.; Jacobson, P. B. *J. Med. Chem.* **2004**, *47*, 4213; (b) Link, J. T.; Sorensen, B. K.; Lai, C.; Wang, J.; Fung, S.; Deng, D.; Emery, M.; Carroll, S.; Grynfarb, M.; Goos-Nilsson, A.; von Geldern, T. *Bioorg. Med. Chem. Lett.* **2004**, *14*, 4173.
- Boyer, S. H.; Jiang, H.; Jacintho, J. D.; Reddy, M. V.; Li, H.; Godwin, J. L.; Schulz, W. G.; Cable, E. E.; Hou, J.; Wu, R.; Fujitaki, J. M.; Hecker, S. J.; Erion, M. D. *J. Med. Chem.* **2008**, *51*, 7075.
- Beberitz, G. B.; Beaulieu, V.; Dale, B. A.; Deacon, R.; Duttaroy, A.; Gao, J.; Grondine, M. S.; Gupta, R. C.; Kakmak, M.; Kavana, M.; Kirman, L. C.; Liang, J.; Maniara, W.; Munshi, S. S.; Schuster, F. F.; Stams, T.; Denny, I. S.; Taslimi, P. M.; Vash, B.; Caplan, S. L. *J. Med. Chem.* **2009**, *52*, 6142.
- (a) Koltun, D. O.; Zilbershtein, T. M.; Migulin, V. A.; Vasilevich, N. I.; Parkhill, E. Q.; Glushkov, A. I.; McGregor, M. J.; Brunn, S. A.; Chu, N.; Hao, J.; Mollova, N.; Leung, K.; Chisholm, J. W.; Zablocki, J. *Bioorg. Med. Chem. Lett.* **2009**, *19*, 4070; (b) Koltun, D. O.; Vasilevich, N. I.; Parkhill, E. Q.; Glushkov, A. I.; Zilbershtein, T. M.; Mayboroda, E. I.; Boze, M. A.; Cole, A. G.; Henderson, I.; Zautke, N. A.; Brunn, S. A.; Chu, N.; Hao, J.; Mollova, N.; Leung, K.; Chisholm, J. W.; Zablocki, J. *Bioorg. Med. Chem. Lett.* **2009**, *19*, 3050.
- For a review, see: Erion, M. D.; Bullough, D. A.; Lin, C.-C.; Hong, Z. *Curr. Opin. Invest. Drugs* **2006**, *7*, 109.
- Hoglen, N. C.; Chen, L.-S.; Fisher, C. D.; Hirakawa, B. P.; Groessl, T.; Contreras, P. C. *J. Pharmacol. Exp. Ther.* **2004**, *309*, 634.
- Boyer, S. H.; Sun, Z.; Jiang, H.; Esterbrook, J.; Gómez-Galeno, J. E.; Craig, W.; Reddy, K. R.; Ugarkar, B. G.; MacKenna, D. A.; Erion, M. D. *J. Med. Chem.* **2006**, *49*, 7711.
- (a) Wess, G.; Kramer, W.; Schubert, G.; Enhsen, A.; Baringhaus, K.-H.; Glombik, H.; Müllner, S.; Bock, K.; Kleine, H.; John, M.; Neckermann, G.; Hoffman, A. *Tetrahedron Lett.* **1993**, *34*, 819; (b) Wess, G.; Kramer, W.; Han, X. B.; Bock, K.; Enhsen, A.; Glombik, H.; Baringhaus, K.-H.; Böger, G.; Urmann, M.; Hoffman, A.; Falk, E. *J. Med. Chem.* **1994**, *37*, 3240; (c) Verdine, G. L.; Norimine, Y.; Gude-Rodrigues, L. WO 2007005941 A2.
- (a) Brukert, E.; Hayem, G.; Dejager, S.; Yau, C.; Begaud, B. *Cardiovasc. Drugs Ther.* **2005**, *19*, 403; (b) Baer, A. N.; Wortmann, R. L. *Curr. Opin. Rheumatol.* **2007**, *19*, 67; (c) Tiwari, A.; Bansal, V.; Chugh, A.; Mookhtiar, K. *Expert Opin. Drug Saf.* **2006**, *5*, 651; (d) Athar, H.; Shah, A. R.; Thompson, P. D. *Future Lipidol.* **2006**, *1*, 143; (e) Franc, S.; Dejager, S.; Bruckert, E.; Chauvenet, M.; Giral, P.; Turpin, G. *Cardiovasc. Drugs Ther.* **2003**, *17*, 459.
- (a) Hamelin, B. A.; Turgeon, J. *Trends Pharm. Sci.* **1998**, *19*, 26; (b) Rosenson, R. S.; Tangney, C. C. *JAMA* **1998**, *279*, 1643; See also: (c) Schachter, M. *Fundam. Clin. Pharmacol.* **2004**, *19*, 117; (d) Ho, R. H.; Tirona, R. G.; Leake, B. F.; Glaeser, H.; Lee, W.; Lemke, C. J.; Wang, Y.; Kim, R. B. *Gastroenterology* **2006**, *130*, 1793.
- For a reviews, see: (a) Rodrigues, A. C. *Expert Opin. Drug Metab. Toxicol.* **2010**, *6*, 621; (b) Niemi, M. *Clin. Pharm. Ther.* **2010**, *87*, 130; For a representative example of genetic variant data, see: SEARCH Collaborative Group *N. Eng. J. Med.* **2008**, *359*, 789.
- Bowles, D. M.; Bolton, G. L.; Boyles, D. C.; Curran, T. T.; Hutchings, R. H.; Larsen, S. D.; Miller, J. M.; Park, W. K. C.; Ritsema, K. G.; Schineman, D. C. *Org. Process Res. Dev.* **2008**, *12*, 1183.
- Baumann, K. L.; Butler, D. E.; Deering, C. F.; Mennen, K. E.; Millar, A.; Nanninga, T. N.; Palmer, C. W.; Roth, B. D. *Tetrahedron Lett.* **1992**, *33*, 2283.
- For a full description of in vitro and in vivo biological assays as well as experimental conditions, see Ref. 2e.
- Duggan, D. E.; Vickers, S. *Drug Metab. Rev.* **1990**, *22*, 333.
- Kalgutkar, A. S.; Feng, B.; Nguyen, H. T.; Frederick, K. S.; Campbell, S. D.; Hatch, H. L.; Bi, Y. A.; Kazolias, D. C.; Davidson, R. E.; Mireles, R. J.; Duignan, D. B.; Choo, E. F.; Zhao, S. X. *Drug Metab. Dispos.* **2007**, *35*, 2111.
- McTaggart, F.; Buckett, L.; Davison, R.; Holdgate, G.; McCormick, A.; Schneck, D.; Smith, G.; Warwick, M. *Am. J. Cardiol.* **2001**, *87*, 23B.
- (a) Parker, T. S.; McNamera, D. J.; Brown, C.; Garrigano, O.; Kolb, R.; Batwin, H.; Ahrens, E. H. *Proc. Natl. Acad. Sci.* **1982**, *79*, 3037; (b) Parker, T. S.; McNamara, D. J.; Brown, C. D.; Kolb, R.; Ahrens, E. H.; Alberts, A. W.; Tobert, J.; Chen, J.; De Schepper, P. J. *Clin. Invest.* **1984**, *74*, 795; (c) Yoshida, T.; Honda, A.; Tanaka, N.; Matsuzaki, Y.; He, B.; Osuga, T.; Kobayashi, N.; Ozawa, K.; Miyazaki, H. *J. Chromatogr., B* **1993**, *613*, 185.
- Pfefferkorn, J. A.; Choi, C.; Larsen, S. D.; Auerbach, B.; Askew, V.; Dillon, L.; Hanselman, J. C.; Kowala, M.; Lin, Z.; Lu, G. H.; Robertson, A.; Sekerke, C.; Bakker-Arkema, R.; Barclay, P.; Kindt, E.; Le, V.; Mandema, J. W.; Milad, M. *Pyrazoles as Hepatoselective HMG-CoA Reductase Inhibitors: Discovery and Early Clinical Evaluation of PF-3052334 for the Treatment of Hypercholesterolemia*; 31st National Medicinal Chemistry Symposium; Pittsburgh, PA. June 15–19, 2008.
- Martin, P. D.; Mitchell, P. D.; Schneck, D. W. *Br. J. Clin. Pharmacol.* **2002**, *54*, 472.